Supporting Information for "Effects of mantle composite rheology on plate-like behavior in global-scale mantle convection"

M. Arnould[1,2], T. Rolf[2,3] and A. Manjón Cabeza-Córdoba [2,4,5]

[1]UCBL, ENSL, UJM, CNRS 5276, Laboratoire de Géologie de Lyon - Terre, Planètes, Environnement, Lyon, France

[2]Centre for Earth Evolution and Dynamics, Department of Geosciences, University of Oslo, Blindern, Oslo, Norway

[3]Institute of Geophysics, University of Münster, Germany

[4]Andalusian Earth Sciences Institute, University of Grenada, Spain

[5]Department of Earth Sciences, University College London, UK

Contents of this file

1. Table S1

2. Figures S1 to S6

Additional Supporting Information (Files uploaded separately)

1. Supplementary Movie 1: Spatio-temporal distribution of dislocation creep and mantle velocity field (arrows scaled and colored by magnitude) in a model of mantle convection with composite rheology (same model as Fig. 2c). Blue lines show slabs (isotherm 1375 K) and magenta lines contour plumes (isotherm 2000 K).

————

April 14, 2023, 1:35pm

:

Table S1. Non-dimensional and dimensional model parameters

Parameter	Non-dim. value	Dim. value	Scaling[a]
Mantle thickness (D)	1	2890 km	
Reference gravitational acceleration (g_0)	1	9.81 m s^{-2}	
Reference thermal expansivity (α_0)	1	5×10^{-5} K^{-1}	
Reference density (ρ_0)	1	3300 kg m^{-3}	
Reference diffusivity (κ_0)	1	1×10^{-6} m^2 s^{-1}	
Temperature gradient (ΔT)	1	2500 K	
Surface temperature (T_{top})	0.12	300 K	ΔT
Basal temperature (T_{bot})	1.12	2800 K	ΔT
Reference viscosity (η_0)	1	9.8×10^{21} Pa s	$\frac{\alpha_0 g_0 \rho_0 \Delta T D^3}{\kappa \mathrm{Ra}_0}$
Internal heating rate (H)	30	8.6×10^{-12} W kg^{-1}	$\frac{k_0 \Delta T}{\rho_0 D^2}$
Diffusion creep activation energy (E_{diff})	6	125 kJ mol^{-1}	$R\Delta T$
Diffusion creep activation volume (V_{diff})	3	0.7 cm^3 mol^{-1}	$\frac{R\Delta T}{\rho_0 g_0 D}$
Stress exponent for diffusion creep (n)	0		
Grain-size exponent for diffusion creep (m)	2		
Dislocation creep activation energy (E_{disl})	11	230 kJ mol^{-1}	$R\Delta T$
Dislocation creep activation volume (V_{disl})	$18 - 50$	$4 - 11$ cm^3 mol^{-1}	$\frac{R\Delta T}{\rho_0 g_0 D}$
Stress exponent for dislocation creep (n)	3.5		
Grain-size exponent for dislocation creep (m)	1		
Reference transition stress (σ_0)	$1 - 3 \times 10^3$	$1.2 - 3.5$ MPa	$\frac{\kappa_0 \eta_0}{D^2}$
Maximum viscosity cut-off	10^4	9.8×10^{25} Pa s	
Surface yield stress (σ_{Y_0})	$1 - 20 \times 10^4$	$12 - 234$ MPa	$\frac{\kappa_0 \eta_0}{D^2}$
Yield stress gradient ($d\sigma_Y$)	0.01	0.325 MPa km^{-1}	$\frac{Ra_0}{\alpha_0 \Delta T} \frac{\kappa_0 \eta_0}{D^3}$

[a] The scaling factors listed in this column need to be multiplied by the non-dimensional values to get the dimensional parameters. $\mathrm{Ra}_0 = 10^7$ is the reference Rayleigh number, $R = 8.314$ kJ mol^{-1} is the gas constant and $k_0 = 3.15$ W m^{-1} K^{-1} is the reference thermal conductivity. Velocities are dimensionalized using D and the thermal diffusion time ($\tau = \frac{D^2}{\kappa}$).
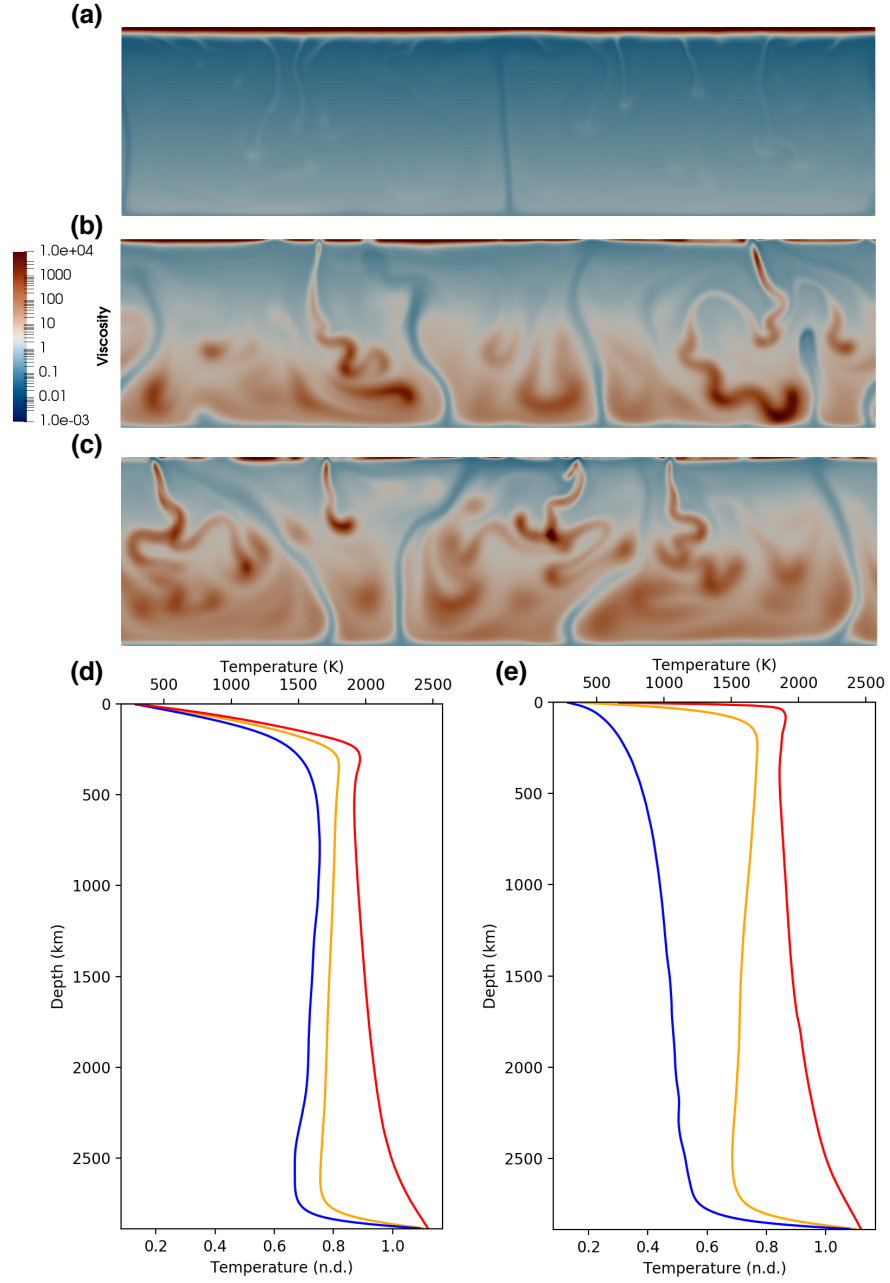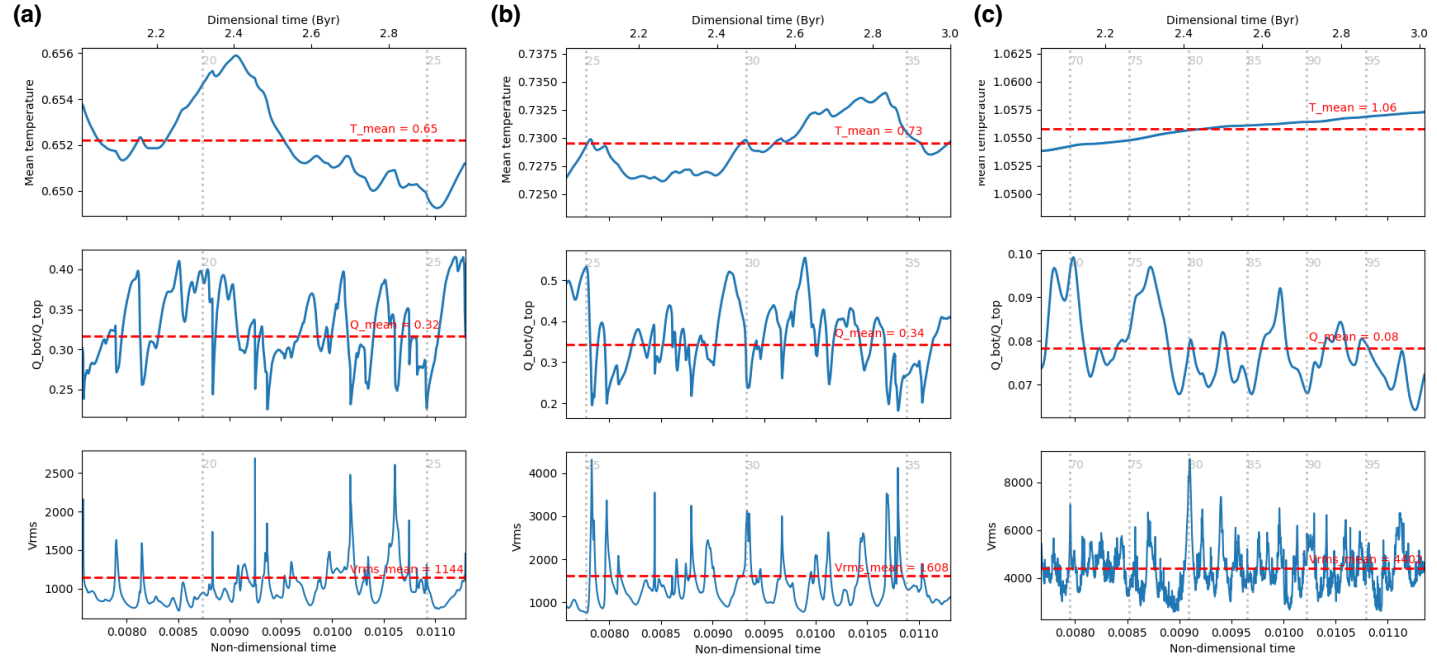
April 14, 2023, 1:35pm

Figure S1. Snapshots (a-b-c) of the viscosity fields of three 2D-cartesian models with different yield stresses (σ_{Y_0} equal to 234 MPa, 47 MPa and 12 MPa respectively), deforming in diffusion creep only. (d) and (e) show the time-averaged temperature profiles of (a) and (b) respectively. The blue, yellow and red curves correspond to the time-averaged minimum, mean and maximum temperature profiles. (a) and (d) correspond to a stagnant-lid model while (b), (c) and (e) correspond to mobile-lid models with plate-like behavior.

Figure S2. Time series of non-dimensional temperature, bottom/surface heat flow ratio and rms velocities for models (a) with $\sigma_{Y_0} = 12$ MPa, $V_{disl} = 11$ cm^3/mol and $\sigma_0 = 3.5$ MPa, (b) $\sigma_{Y_0} = 35$ MPa, $V_{disl} = 11$ cm^3/mol and $\sigma_0 = 3.5$ MPa, and (c) $\sigma_{Y_0} = 234$ MPa, $V_{disl} = 4$ cm^3/mol and $\sigma_0 = 3.5$ MPa. The red line corresponds to the average of each time series. The dotted grey lines represent specific overturns and correspond to the amount of time necessary for a particle to sink from the surface to the base of the mantle and then back to the surface at the average rms velocity of the corresponding model. Non-dimensional time is dimensionalized using diffusivity: $t_{dim} = t * \times \frac{D^2}{\kappa_0}$.
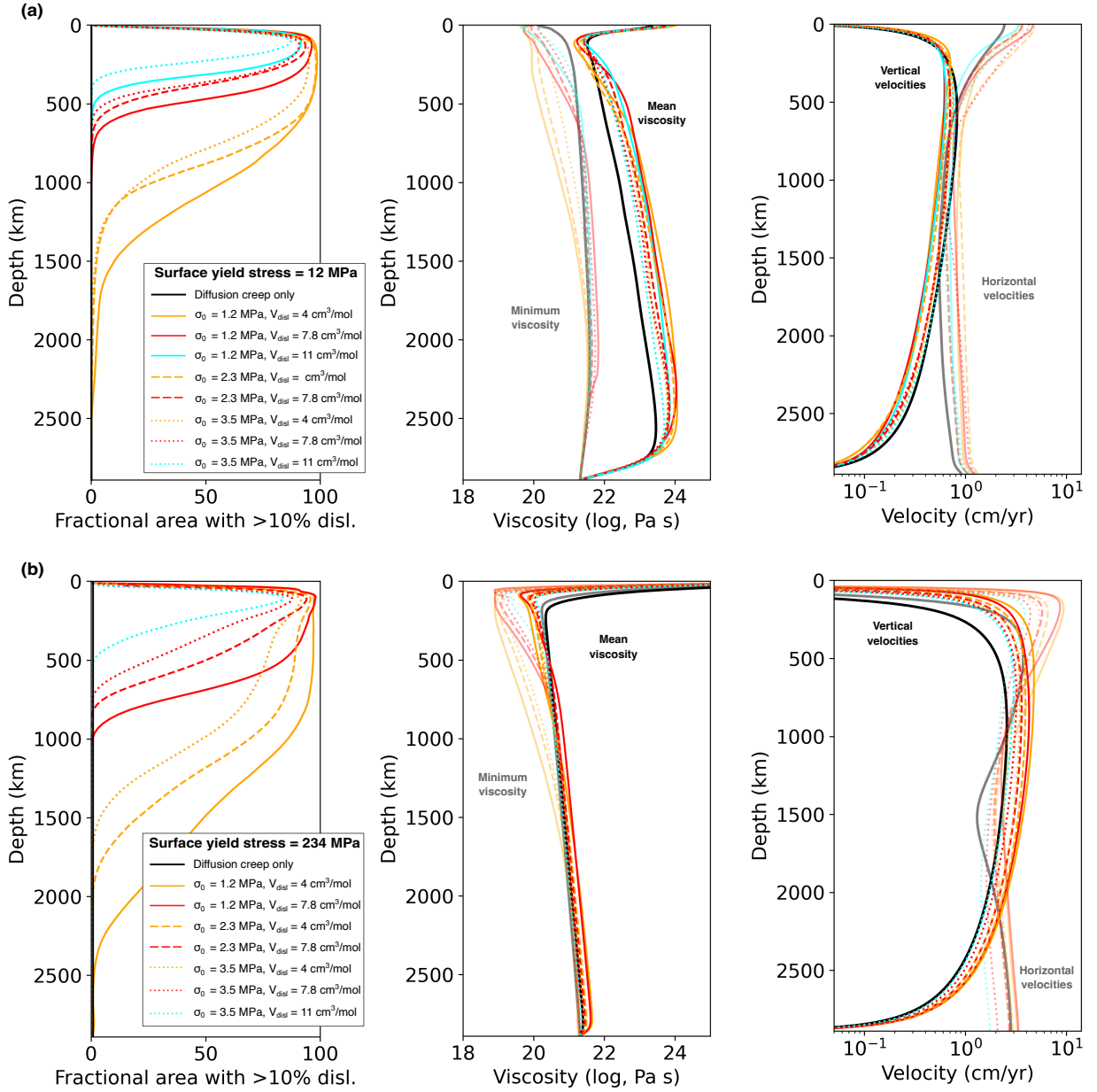
Figure S3. Same depth-profiles as Fig. 2a, but (a) for a low surface yield stress), and (b) for a high surface yield stress. Although the absolute values of viscosity change with the surface yield stress for model in pure diffusion creep due to regime transition from mobile lid (cool and viscous) at 12 MPa to stagnant lid (hot) at 234 MPa, accounting for different amounts of dislocation creep generally has a lowering effect on mantle viscosity.
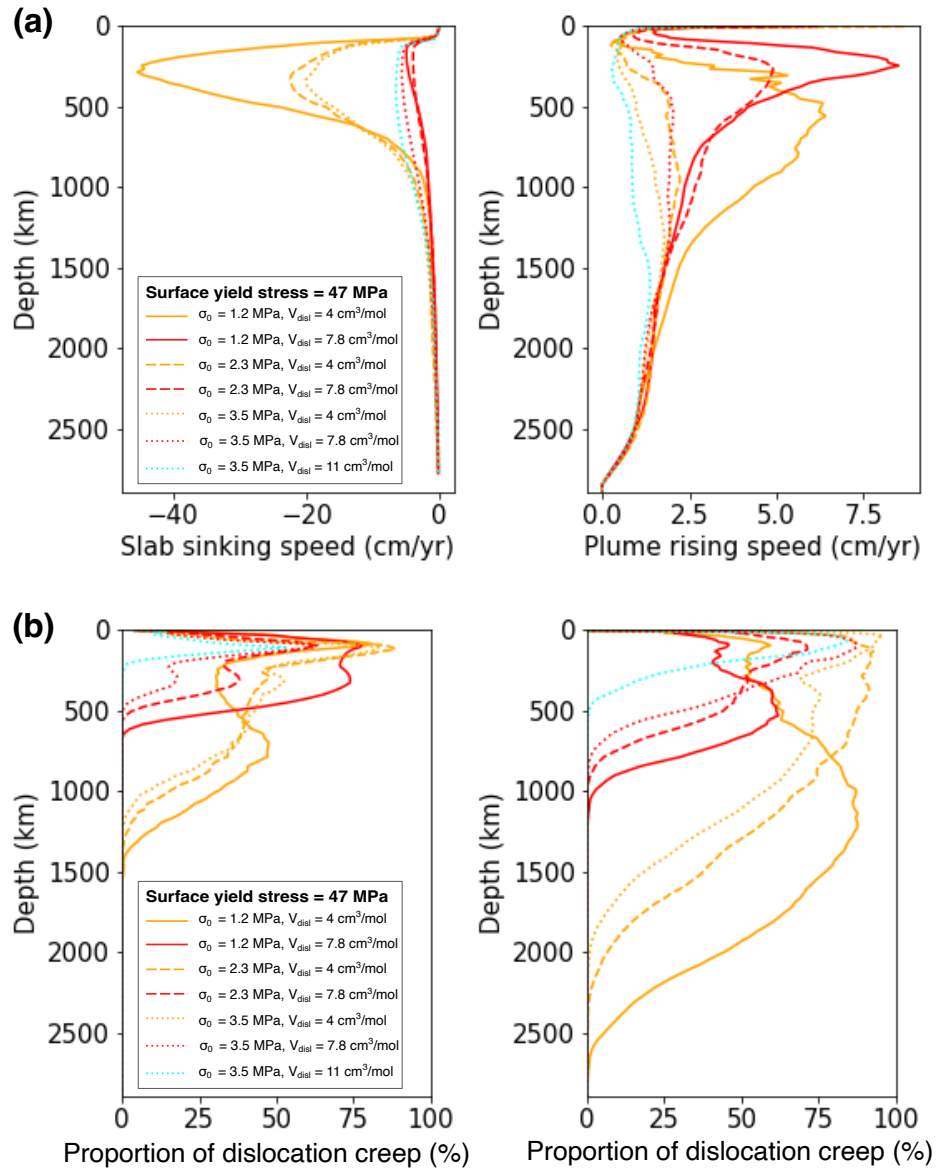
April 14, 2023, 1:35pm

Figure S4. Rheological properties and behavior inside slabs (left panels) and plumes (right panel) in composite rheology models with a surface yield stress of 47 MPa. Time-averaged depth profiles of (a) sinking/rising speed and (b) proportion of slab/plume material deforming through dislocation creep. Note the increasing vertical velocity with increasing proportion of dislocation creep.
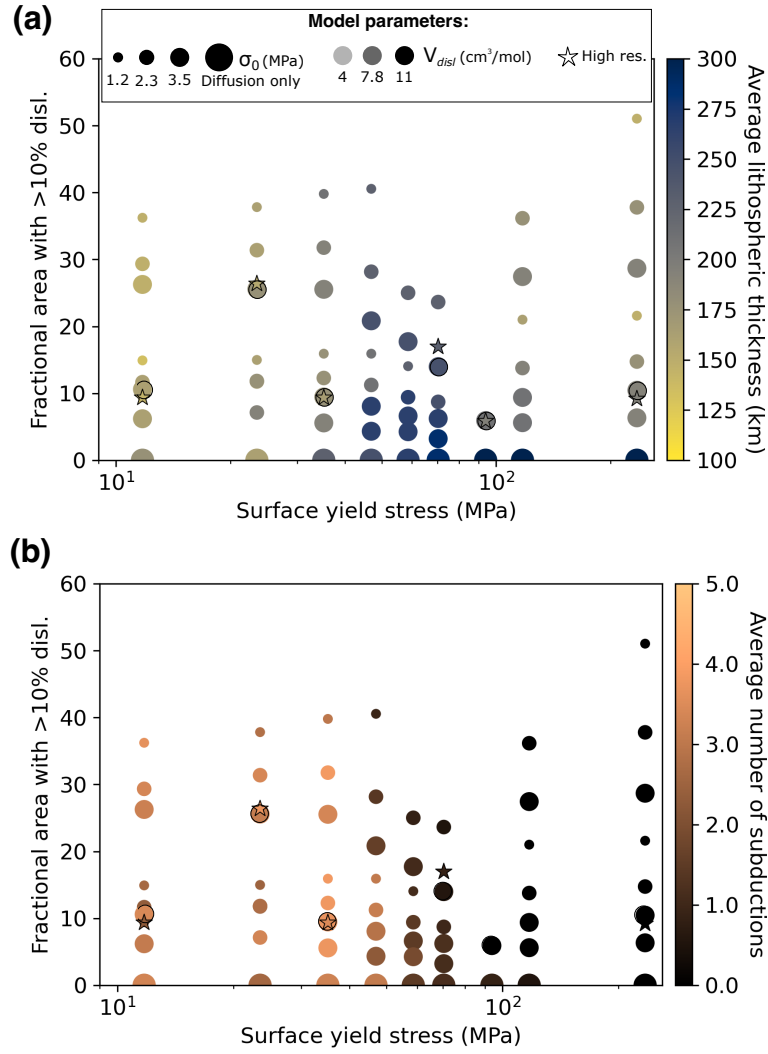
Figure S5. Regime diagram as shown on Figure 4 of the main manuscript, but with colours referring to (a) time-averaged lithosphere thickness and (b) to the average number of subductions. Note the progressive increase of lithospheric thickness in models in pure diffusion creep as the surface yield stress increases. Also note that for a given surface yield stress, the increase in the mantle fractional area containing more than 10 % dislocation creep leads to progressive lithosphere thinning. Models with a surface yield stress lower than 50 MPa tend to exhibit more subductions when increasing the amount of mantle deforming through dislocation creep compared to models with diffusion creep only.
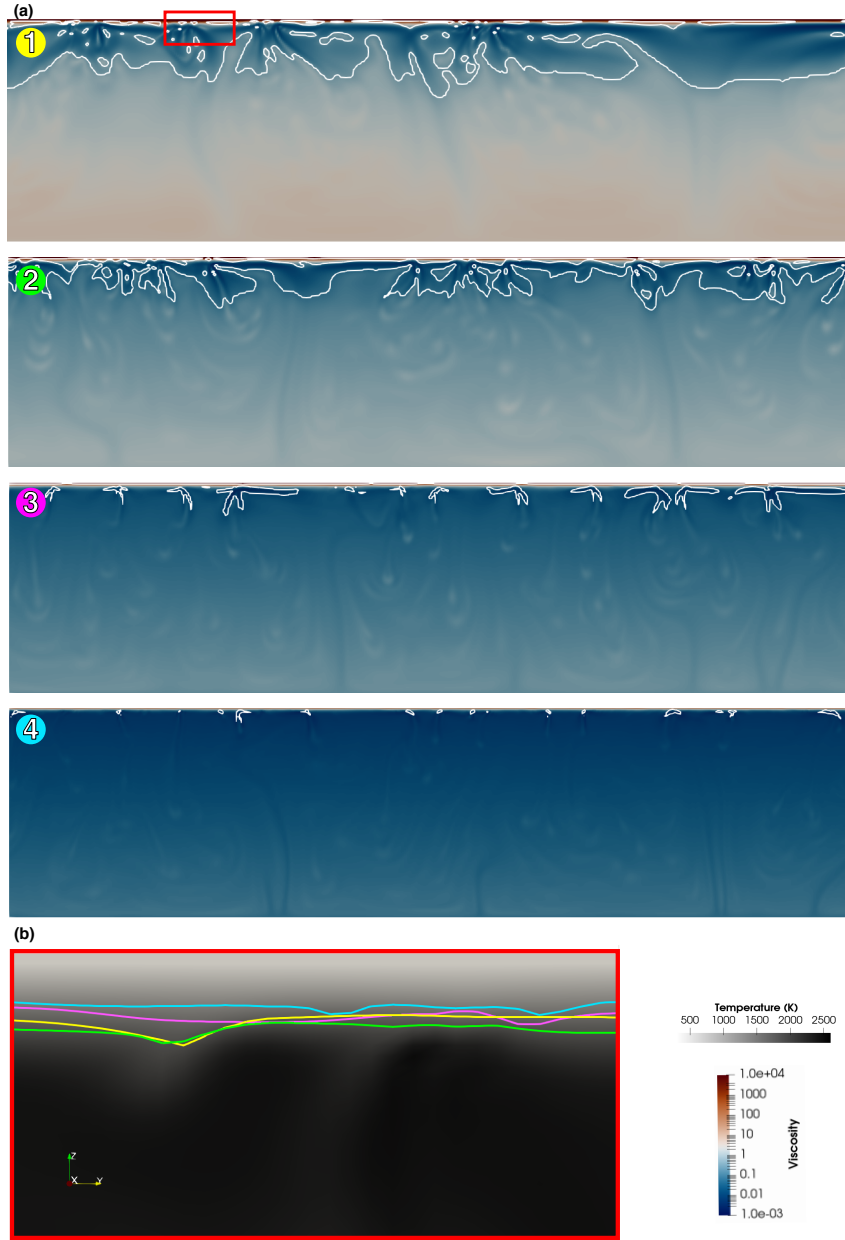
Figure S6. Effect of static grainsize on the planform of convection, on the proportion of dislocation creep and on the lithospheric thickness in stagnant-lid models. (a) Snapshots of the viscosity field for 4 models with composite rheology ($V_{disl} = 7.8$ cm^3 mol^{-1} and $\sigma_0 = 3.5$ MPa). In models 1, 2, and 4 the grain size is 4x, 2x, and 0.5x the grain size in model 3, respectively. White lines contour low-viscosity areas deforming 100% in dislocation creep. (b) Zoom in on the temperature field of Model 1 (red square on (a.1)) showing the location of the isotherm 1700 K for all models at the end of the simulations.